University of Reading

Sub-auroral heating at Jupiter following a solar wind compression

Article

Published Version

Creative Commons: Attribution 4.0 (CC-BY)

Open Access

O'Donoghue, J. ORCID: https://orcid.org/0000-0002-4218-1191, Moore, L., Melin, H., Stallard, T., Kurth, W. S., Owens, M. ORCID: https://orcid.org/0000-0003-2061-2453, Bhakyapaibul, T., Tao, C., Connerney, J. E. P., Knowles, K. L., Kita, H., Roberts, K., Tiranti, P. I., Agiwal, O., Johnson, R., Wang, R., Thomas, E. and Murakami, G. (2025) Sub-auroral heating at Jupiter following a solar wind compression. Geophysical Research Letters, 52 (7). e2024GL113751. ISSN 1944-8007 doi: 10.1029/2024GL113751 Available at https://centaur.reading.ac.uk/122240/

It is advisable to refer to the publisher's version if you intend to cite from the work. See Guidance on citing.

To link to this article DOI: http://dx.doi.org/10.1029/2024GL113751

Publisher: American Geophysical Union

All outputs in CentAUR are protected by Intellectual Property Rights law, including copyright law. Copyright and IPR is retained by the creators or other copyright holders. Terms and conditions for use of this material are defined in the End User Agreement.

University of Reading

www.reading.ac.uk/centaur

CentAUR

Central Archive at the University of Reading

Reading's research outputs online

Check for updates

Geophysical Research Letters

RESEARCH LETTER
10.1029/2024GL113751

Sub-Auroral Heating at Jupiter Following a Solar Wind Compression

James O'Donoghue[1,2], L. Moore[3], H. Melin[4], T. Stallard[4], W. S. Kurth[5], M. Owens[1], T. Bhakyapaibul[6], C. Tao[7], J. E. P. Connerney[8,9], K. L. Knowles[4], H. Kita[10], K. Roberts[3], P. I. Tiranti[4], O. Agiwal[3], R. Johnson[11], R. Wang[12], E. Thomas[4], and G. Murakami[2]

[1]Department of Meteorology, University of Reading, Reading, UK, [2]Institute of Space and Astronautical Science, Japan Aerospace Exploration Agency, Sagamihara, Japan, [3]Center for Space Physics, Boston University, Boston, MA, USA, [4]Department of Mathematics, Physics and Electrical Engineering, Northumbria University, Newcastle-upon-Tyne, UK, [5]Department of Physics and Astronomy, University of Iowa, Iowa City, IA, USA, [6]The Grainger College of Engineering, University of Illinois Urbana-Champaign, Urbana, IL, USA, [7]National Institute of Information and Communications Technology (NICT), Tokyo, Japan, [8]NASA Goddard Space Flight Center, Greenbelt, MD, USA, [9]Space Research Corporation, Annapolis, MD, USA, [10]Tohoku Institute of Technology, Sendai, Japan, [11]Department of Physics, Aberystwyth University, Aberystwyth, UK, [12]School of Physics and Astronomy, University of Leicester, Leicester, UK

Abstract Jupiter's polar aurorae deliver significant heating at the poles, thought to spread across the planet through atmospheric winds. Additionally, ground-based Keck observations have revealed a large-scale high-temperature region, spatially distinct from the aurorae. Here, we investigate the origins and characteristics of the feature using Keck data, in-situ Juno spacecraft measurements, and solar wind modeling. Juno exited the magnetosphere on approach to Jupiter, coinciding with modeled high-speed solar wind impact that compressed the magnetosphere. This hot feature may be dynamic, transported equatorward by winds following auroral activity enhancements from magnetospheric compression akin to a large-scale traveling ionospheric disturbance on Earth, or driven by the inner magnetosphere particle precipitation. Exploring the dynamic case, we calculated equatorward velocities ranging from 0.46 to 2.02 km s^{-1}, similar to those seen at Earth. Our study underscores the importance of the solar wind at all planets, exemplified by its ability to alter Jupiter's upper-atmospheric energy balance globally.

Plain Language Summary Jupiter's powerful aurorae release vast amounts of energy into the planet's upper atmosphere, primarily in the polar regions. Normally, temperatures decrease gradually toward the equator, reflecting how auroral energy is redistributed across the planet. However, a recent discovery revealed a large, high-temperature region far from the aurorae, disrupting this typical pattern. In this study, data from NASA's Juno spacecraft and solar wind models indicate that strong solar winds likely compressed Jupiter's magnetic field several hours before this hot region appeared. This compression may have intensified auroral heating, driving the hot region away from the auroral zone. Alternatively, the region could have been heated by a yet unknown process. In either case, prior solar wind activity appears to have been the key trigger.

Key Points:

- Jupiter's sub-auroral upper-atmospheric temperature was seen 200 K elevated in a region measuring 180° longitude by 8° latitude
- Juno data and solar wind modeling demonstrate that the Jovian magnetosphere was compressed several hours prior by fast solar wind streams
- The hot feature may drift equatorward from the aurora at 1.1 ± 0.2 km s^{-1}, or be driven by a novel magnetospheric energy source

Supporting Information:

Supporting Information may be found in the online version of this article.

Correspondence to:

J. O'Donoghue,
james.odonoghue@reading.ac.uk

Citation:

O'Donoghue, J., Moore, L., Melin, H., Stallard, T., Kurth, W. S., Owens, M., et al. (2025). Sub-auroral heating at Jupiter following a solar wind compression. *Geophysical Research Letters*, *52*, e2024GL113751. https://doi.org/10.1029/2024GL113751

Received 17 NOV 2024
Accepted 6 MAR 2025

Author Contributions:

Conceptualization: James O'Donoghue
Data curation: James O'Donoghue, L. Moore, W. S. Kurth, J. E. P. Connerney, K. Roberts
Formal analysis: James O'Donoghue, T. Stallard
Funding acquisition: James O'Donoghue
Investigation: James O'Donoghue, L. Moore, H. Melin, T. Stallard, W. S. Kurth, M. Owens, T. Bhakyapaibul, C. Tao, J. E. P. Connerney, K. L. Knowles, H. Kita, K. Roberts, P. I. Tiranti, O. Agiwal, R. Johnson, R. Wang, E. Thomas, G. Murakami
Methodology: James O'Donoghue, L. Moore

© 2025. The Author(s).
This is an open access article under the terms of the Creative Commons Attribution License, which permits use, distribution and reproduction in any medium, provided the original work is properly cited.

1. Introduction

Jupiter's upper atmosphere begins hundreds of kilometers above the planet's 1-bar pressure surface and may be considered composed of two co-located components: a thermosphere and an ionosphere (Yelle & Miller, 2004). The neutral thermosphere is mainly composed of molecular hydrogen, co-located with an ionosphere composed of electrons and (mainly) H_3^+ and H^+ ions (O'Donoghue & Stallard, 2022; Tao et al., 2011). Escaping neutrals from the volcanic moon Io, in orbit about Jupiter at 5.9 R_J (where 1 R_J is Jupiter's equatorial radius; 71,492 km at 1-bar pressure), become ionized by charge-exchange and solar extreme ultraviolet (UV), populating the Jovian magnetosphere with plasma. However, the 9-hr 56-min rotation period of Jupiter and its magnetosphere partially entrap the plasma, ultimately generating magnetosphere-ionosphere coupling currents which deliver charged-particle precipitation and heating to the polar regions, forming the Jovian aurorae (Cowley et al., 2005). Auroral upper atmospheric temperatures at the magnetic poles of Jupiter are typically over 900 K (Adriani et al., 2017; Johnson et al., 2018; Melin et al., 2006; Moore et al., 2017; T. Stallard et al., 2001), whereas temperatures away from the auroral region are on the order of 700 K (Lam et al., 1997; Melin et al., 2024; Migliorini et al., 2019).

Project administration: James O'Donoghue
Resources: James O'Donoghue, L. Moore, H. Melin, W. S. Kurth, M. Owens, C. Tao, J. E. P. Connerney
Software: James O'Donoghue, L. Moore, H. Melin, M. Owens, T. Bhakyapaibul, C. Tao, J. E. P. Connerney, K. L. Knowles
Supervision: James O'Donoghue
Validation: James O'Donoghue, L. Moore, H. Melin, T. Stallard
Visualization: James O'Donoghue
Writing – original draft: James O'Donoghue
Writing – review & editing: James O'Donoghue, L. Moore, H. Melin, T. Stallard, W. S. Kurth, M. Owens, T. Bhakyapaibul, C. Tao, J. E. P. Connerney, K. L. Knowles, H. Kita, K. Roberts, P. I. Tiranti, O. Agiwal, R. Johnson, R. Wang, E. Thomas, G. Murakami

Polar region temperatures are adequately explained by ion-neutral collisional heating associated with the auroral mechanism, but the remainder of the planet is simulated to be 200 K based on solar heating alone, some 500 K lower than observed (Miller et al., 2020; Strobel & Smith, 1973; Yelle & Miller, 2004). Two main candidate heating mechanisms have been thought to explain these temperatures in recent literature: the dissipation of gravity and acoustic waves traveling from below and/or the global distribution of auroral energy by upper atmospheric circulation. Gravity waves were modeled to either heat or cool the thermosphere by tens of Kelvin, while acoustic waves could heat the region by hundreds of Kelvin (Lian & Yelle, 2019; Matcheva & Strobel, 1999; Walterscheid et al., 2003). The upper atmosphere above Jupiter's Great Red Spot was once measured to be over 1,600 K and was interpreted as a signature of acoustic wave heating (O'Donoghue et al., 2016), but subsequent observations have not shown a significant temperature enhancement in the region, which may indicate that such heating is time-variable (Melin et al., 2024; O'Donoghue et al., 2021).

A redistribution of auroral energy has long been proposed to explain this discrepancy, requiring that the hot upper atmosphere from the magnetic polar regions continuously propagates toward the equator through a system of winds. Bougher et al. (2005) demonstrated this process using a global circulation model (GCM) at Jupiter. Observations of auroral temperature measured by H_3^+—a proxy for neutral upper atmosphere temperatures (Miller et al., 2006)—found that auroral temperatures fall off too quickly over time to be explained by radiative cooling alone, supportive of the idea that polar heat is transported away (Melin et al., 2006). However, subsequent GCM studies for Jupiter and Saturn showed that efficient heat redistribution was unlikely, as Coriolis forces associated with intense zonal winds on these rapidly rotating planets deflect meridional flows, effectively confining heat near the poles (Smith et al., 2007; Yates et al., 2020).

Recently, two longitude-latitude maps of Jupiter's upper atmosphere temperatures were produced with ground-based Keck telescope observations of H_3^+ (O'Donoghue et al., 2021). The two maps, recorded in 2016 and 2017, show a temperature gradient in which high polar temperatures gradually diminish to lower temperatures at the equator, consistent with the idea that hot auroral atmosphere is able to escape to lower latitudes, in spite of the zonal flows which ought to resist them. While temperature gradients help to confirm global energy transport and its direction (on average), a useful next step to improve our understanding of this mechanism is to measure the velocity of the flows planet-wide. In the auroral regions, velocities of hundreds of $m\ s^{-1}$ were measured using Doppler-shifted H_3^+ lines with a spectral resolution of $R \sim 100{,}000$ (Johnson et al., 2018). High spectral resolution and signal to noise enable sub-pixel precision here, but outside the aurora, where lines are an order of magnitude fainter, such measurements are difficult.

The 2017 temperature map of O'Donoghue et al. (2021) reported on the presence of a large hot feature (up to 950 K above a background of 750 K) far from the auroral region, which extends 160° in longitude around the planet. There are no known heating mechanisms capable of producing a feature with these temperatures outside of the auroral region, so it was hypothesized that the feature was launched toward the equator from the main auroral oval. A rapid increase in auroral heating may facilitate such a launch, as the resultant adiabatic expansion of the upper atmosphere would lead to winds which transport hot gases away from the main auroral oval, which is often seen in Earth's upper atmosphere (Palmroth et al., 2021). Assuming an auroral origin, a growing distance between the feature's center and the main oval was measured throughout the several-hour observing sequence, from which the feature's median equatorward velocity was derived to be 620 m s^{-1}. However, this single, simplistic estimate was only based on a growing latitudinal distance between the feature and the main oval at the same longitudes and did not include the possibility of longitudinal drift.

The cause of the sudden auroral heating itself was thought to be due to a solar wind compression of the Jovian magnetosphere, as global circulation modeling work predicted extended regions of equatorward flow in this scenario (Yates et al., 2014). Indeed, modeled solar wind dynamic pressure at Jupiter was estimated to be an order of magnitude higher than in the several days preceding the Keck observation on 25 January 2017, but the arrival time uncertainty was a wide ±1.5 days. If this feature has a solar wind driver, it adds to growing evidence that the Jovian aurorae and the global upper atmosphere at large are strongly affected by conditions in the solar wind, despite the system being driven internally (Baron et al., 1996; Bonfond et al., 2020; Moore et al., 2017). Uncertainties in solar wind arrival times and the dynamics of the hot feature–assuming it is indeed moving–have limited our ability to draw definitive conclusions about the origin and underlying physics of this important mechanism. In this study, we incorporate new data from the Juno spacecraft which reveals the state of the Jovian magnetosphere, providing updated estimates for solar wind conditions at Jupiter. Furthermore, we explore the

19448007, 2025, 7, Downloaded from https://agupubs.onlinelibrary.wiley.com/doi/10.1029/2024GL113751 by Test, Wiley Online Library on [05/04/2025]. See the Terms and Conditions (https://onlinelibrary.wiley.com/terms-and-conditions) on Wiley Online Library for rules of use; OA articles are governed by the applicable Creative Commons License

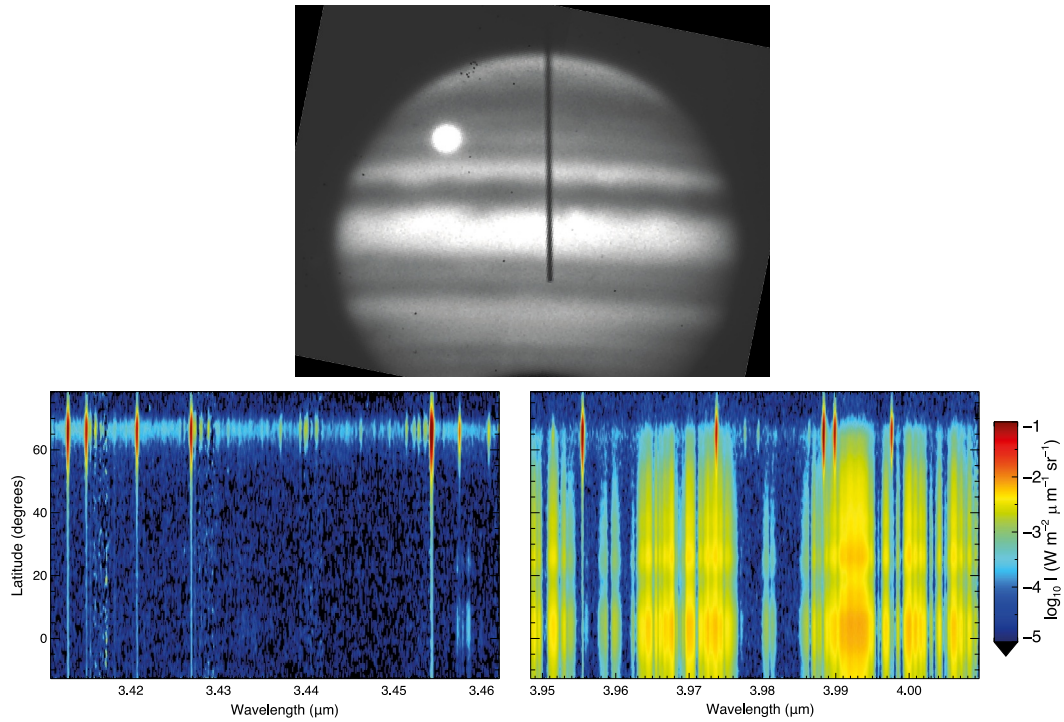

Figure 1. An example Keck NIRSPEC slit-viewing camera image (top) and spectral image (bottom) recorded on 25 January 2017 at 11:42 UT. (top) A guide-camera image of Jupiter filtered between 2.134 and 4.228 μm, used to indicate the position of the slit relative to Jupiter, which is fixed to local noon throughout the observations. Bright regions mainly correspond with reflected sunlight from ammonia cloud decks and polar hazes, while the satellite Europa can also be seen on the top left. (bottom) A spectral image of Jupiter divided into two orders showing spectral radiance versus wavelength and planetocentric latitude. Methane absorbs sunlight strongly at shorter wavelengths (left), while reflected sunlight dominates at longer wavelengths (right). H_3^+ emission lines are present in both spectral orders, vertically extending from the north pole (and above the planet) to just-south of the equator.

hypothesis that the feature is dynamically moving by deriving precise velocities across all longitudes, which also returns an estimated launch time for the feature.

2. Observations

Here, we re-interpreted observations originally presented in O'Donoghue et al. (2021). On 25 January 2017, between 11:36 and 16:28 Universal Time (UT), Jupiter's upper-atmospheric H_3^+ rotational-vibrational emissions were observed in the near-infrared (3–4 μm) by the 10-m Keck II telescope with its R ∼ 25,000 spectral resolution spectrometer, NIRSPEC (Near-InfraRed Spectrometer) (McLean et al., 1998). The NIRSPEC slit, measuring 24″ × 0.432″, was aligned from north pole to equator along Jupiter's rotational axis as shown in Figure 1 (top) by an example NIRSPEC slit-viewing camera image. These images were taken every 9 s in order to ascertain the changing position of the slit in front of the planet during the night, while spectral images, such as that shown in Figure 1 (bottom), were simultaneously recorded for the spectral analysis of H_3^+ emission lines, with each exposure lasting 60-s. Calibration and other overheads meant that exposures were captured on Jupiter's noon meridian every 3.4 min, during which the planet rotated 2.3°. These observations were astronomically reduced and mapped to produce a data cube of H_3^+-containing emissions for Jupiter's entire northern hemisphere between 120 and 330° longitude, a process described in more detail in O'Donoghue et al. (2021).

From this data cube, the intensity ratio of two H_3^+ emission lines, one at 3.41277 μm and one at 3.9529 μm, were fitted using a model of the ion in order to determine three key H_3^+ parameters: column-averaged temperature, radiance (also known as the total emission) and line-of-sight corrected column-integrated density. The model and the fits it produced for the present work were reported by O'Donoghue et al. (2021), so the procedures are only

19448007, 2025, 7, Downloaded from https://agupubs.onlinelibrary.wiley.com/doi/10.1029/2024GL113751 by Test, Wiley Online Library on [05/04/2025]. See the Terms and Conditions (https://onlinelibrary.wiley.com/terms-and-conditions) on Wiley Online Library for rules of use; OA articles are governed by the applicable Creative Commons License

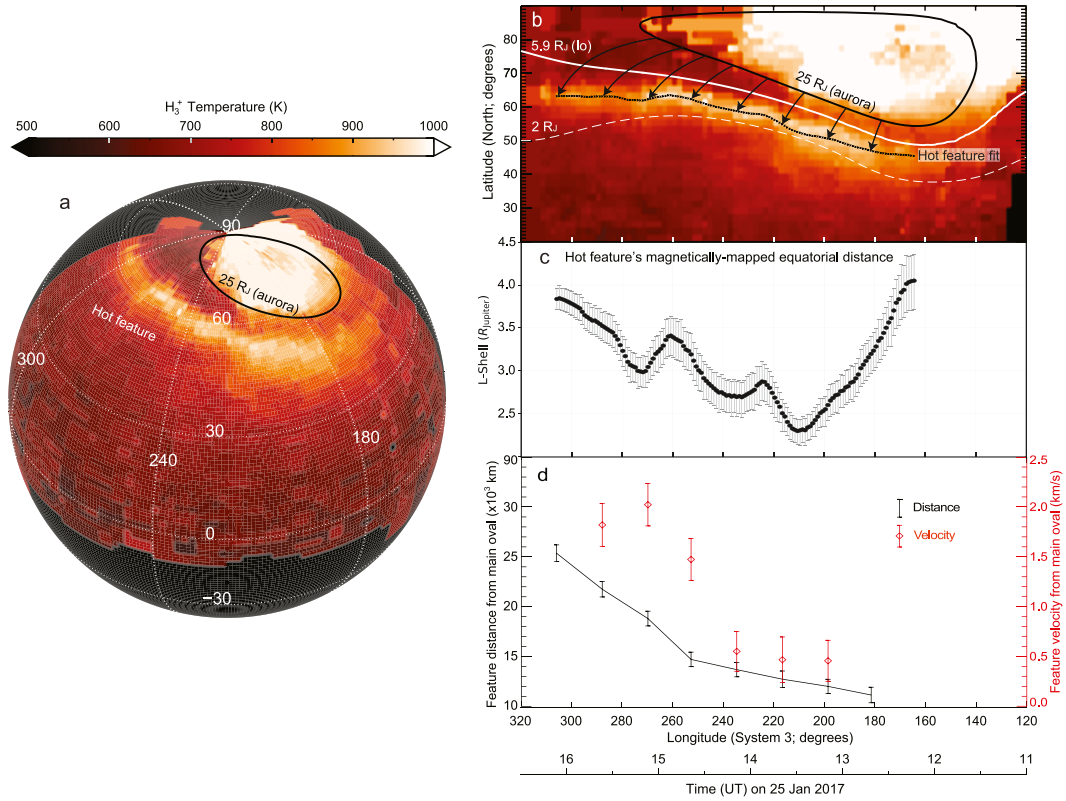

Figure 2. Map projections of H_3^+ temperatures with analyses of the sub-auroral hot feature, all recorded at local noon on the planet. Panel a displays temperatures as a function of longitude and latitude, with the main auroral oval outlined in solid black. This oval corresponds to regions magnetically mapped along field lines to a distance of 25 R_J in Jupiter's equatorial plane. Panel b displays an equirectangular projection of a portion of panel a with the fit to the center of the hot feature. Here, the hot feature is connected to its nearest neighbors (along a great circle) to the auroral oval by black arrows, while magnetic footprints are overlaid and marked at equatorial distances of 5.9 R_J (Io's orbit) and 2.0 R_J. Panel c indicates where in the equatorial magnetosphere the hot feature traces to, in terms of Jupiter radii (L-shell). Panel d presents the distance between the hot feature and the oval, where velocities are calculated by dividing the change in distance by the time interval between data points. Six velocities are obtained using pairs separated by one intermediate data point; an example is given in the main text, with details of the magnetic field model used. Error bars in panels b and d derive from the telescope pointing errors and atmospheric seeing. Panel b is re-plotted in Figure S4 in Supporting Information S1 so as to provide an unobstructed view of the hot feature.

briefly discussed here. While more emission lines are present in the data, these two were found to be considerably less affected by emissions from other species at all latitudes. The H_3^+ model itself, based in the *Interactive Data Language* (IDL) programming language, has been used in numerous prior studies (Melin et al., 2014, 2016; O'Donoghue et al., 2014; T. S. Stallard et al., 2018) and now has an open-source Python-language counterpart (*h3ppy*; https://github.com/henrikmelin/h3ppy). Four example fits to the ion, along with corresponding temperatures and uncertainties, are shown in Figure S1 in Supporting Information S1.

3. Results and Discussion

On the night of 25 January 2017, a total of five maps were generated for each of the three H_3^+ parameters. The temperature map is projected in Figure 2 and has an overall median uncertainty of 1.6%. The full maps for H_3^+ density and emission are shown in Figure S2 in Supporting Information S1. The location of Jupiter's main auroral oval is overlaid in Figures 2a and 2b, connected by Jupiter's magnetic field to 25 R_J in the equatorial plane. Additional magnetic mappings to 5.9 R_J (Io's orbit) and 2.0 R_J are included for reference. This mapping used the JRM33 internal magnetic field model (Connerney et al., 2022) with an external model for Jupiter's magnetodisc

19448007, 2025, 7, Downloaded from https://agupubs.onlinelibrary.wiley.com/doi/10.1029/2024GL113751 by Test, Wiley Online Library on [05/04/2025]. See the Terms and Conditions (https://onlinelibrary.wiley.com/terms-and-conditions) on Wiley Online Library for rules of use; OA articles are governed by the applicable Creative Commons License

("Con2020") (Connerney et al., 2020), and was generated using the open-source JupiterMag code in Python (version 1.3.1, to degree 13) (Wilson et al., 2023). The precipitation of charged particles occurs mainly along and within the main oval, producing H_2^+ which, by the reaction $H_2 + H_2^+ \rightarrow H_3^+ + H$, leads to high H_3^+ densities along the oval seen in Figure S2 in Supporting Information S1 (Miller et al., 2010). Temperatures in the polar region are elevated on and inside the main oval, indicating that auroral heating is not well confined to the oval; a result seen in previous studies (Johnson et al., 2018). A high temperature feature is evident, covering approximately 180° of longitude and several degrees of latitude, displaced far equatorward of the main auroral oval (solid black). There are two distinct hypotheses for its origin that we explore in this section: either it is imposed by the magnetosphere locally and therefore stationary on the planet itself, or it is dynamic, transported to the region from the auroral region.

In the stationary case, we suggest that the feature could be driven by forcing from the innermost Jovian magnetosphere and/or radiation belts, potentially through mid-latitude particle precipitation or a current system causing Joule heating. Precipitation is occurring in this region, as observed remotely by Juno in UV Gladstone et al. (2017) and in situ through measurements of electron density enhancements (Kurth et al., 2025). Cowley et al. (2005) estimated Jovian global upper-atmospheric heating contributions of 1 TW from solar UV, 4–8 TW from particle precipitation, and 600 TW from auroral-zone Joule heating. While particle precipitation can contribute to heating, it may not be sufficient to produce the auroral-like heating required to explain the planetary-scale hot feature seen here. Furthermore, Figure S2 in Supporting Information S1 shows evidence that H_3^+ density is not elevated and even slightly decreased along the feature, whereas localized particle precipitation would be expected to increase it. An alternative explanation may be that precipitation preferentially falls at high altitudes here, enhancing H_3^+ production where upper-atmospheric temperatures are highest, thus weighting our column-integrated emission measurements toward hotter regions. However, under this scenario, H_3^+ production should still exceed the solar-produced background level.

An associated electric current system delivering Joule heating may instead explain the hot feature, akin to the aurorae but temporary, as it has only been observed on one night to date. This current system, or the previously discussed preferentially high-altitude precipitation, could be sustained by Jupiter's ionospheric dynamo through complex vertical and horizontal drifts within the ionosphere (Kurth et al., 2025). Figure 2c illustrates where the feature maps to in Jupiter's equatorial plane via magnetic field lines, suggesting either that the magnetospheric source region (if it is indeed the source) is broad or moves rapidly, on the order of tens of km s^{-1}. The lack of a well-defined theoretical source region, coupled with the fact that the hot feature spans half the planet without interruption, leads us to consider a dynamic explanation in which hot atmosphere has traveled from the aurorae to this position. It is possible that the hot feature we see on Jupiter is essentially a manifestation of a large-scale traveling ionospheric disturbance seen on Earth. These occur when a sudden auroral heating increases ion temperatures, which expands the thermosphere, and drives winds away from the region (Borries et al., 2017). The expansion also lifts heavier molecules (O_2, N_2), increasing recombination rates and reducing total electron content; if hydrocarbons reach higher altitudes at Jupiter under the same mechanism, it may quench H_3^+ and other ions, and may therefore explain the slight H_3^+ reduction seen in Figure S2 in Supporting Information S1.

Figures 2a and 2b show increasing separation between the feature and auroral oval over time, enabling velocity measurement under the assumption of auroral origin. In the prior study on this data set, only the latitudinal differences between this feature were measured at each longitude, using the (older) JRM09 magnetic field model of Connerney et al. (2018); O'Donoghue et al. (2021). Here, distances are determined by selecting longitudinal positions along the hot feature's latitudinal central position (obtained using Gaussian fits shown in Figure 2b), before connecting them to the main oval by the shortest ("great circle") route at several locations. The nearest-neighbor vectors show flows advancing south-west from the main oval, though this is expected given the geometry of the oval at the longitudes covered and the strong westward zonal winds. Using Newton's Method for solving the inverse geodesic problem and accounting for the oblateness of Jupiter (Karney, 2013), eight distances between the main oval and the hot feature were determined, as illustrated in Figure 2d. With increasing longitude, the feature moves further from the oval: the change in the distance between any two data points is divided by the change in time between them, allowing for the calculation of velocity. To reduce positional uncertainties in our estimate of velocity, we selected distance/data pairs separated by one intermediate value to cover more longitudes. For example, the feature moved 1,588 km between 182 and 217° longitude, while 58 min elapsed, leading to a velocity of 0.46 km s^{-1}.

19448007, 2025, 7, Downloaded from https://agupubs.onlinelibrary.wiley.com/doi/10.1029/2024GL113751 by Test, Wiley Online Library on [05/04/2025]. See the Terms and Conditions (https://onlinelibrary.wiley.com/terms-and-conditions) on Wiley Online Library for rules of use; OA articles are governed by the applicable Creative Commons License

19448007, 2025, 7, Downloaded from https://agupubs.onlinelibrary.wiley.com/doi/10.1029/2024GL113751 by Test, Wiley Online Library on [05/04/2025]. See the Terms and Conditions (https://onlinelibrary.wiley.com/terms-and-conditions) on Wiley Online Library for rules of use; OA articles are governed by the applicable Creative Commons License

Dividing a distance from the oval at each longitude in Figure 2d by a velocity, we produce an estimate for its launch time. The overall mean velocity of the feature is 1.1 ± 0.2 km s^{-1}, which implies an average launch time for the whole feature of 10: $24^{+33\text{min}}_{-55\text{min}}$ UT on 25 January. The average of the three highest-longitude velocities is 1.8 ± 0.2 km s^{-1}, giving an average launch time for the feature *in this location* of 12: $14^{+19\text{min}}_{-24\text{min}}$ UT on 25 January, which may explain the hot region near to the auroral oval at 130° longitude (recorded at 11:45 UT) and 80° latitude in Figure 2. The average value for the three velocities at the lowest longitudes is 0.49 ± 0.2 km s^{-1}, giving an average launch time of 06: $24^{+2.2hr}_{-5.7hr}$ UT on 25 January. Figure S3 in Supporting Information S1 displays these values individually for close inspection, and we note that as the perimeter of the feature extends equatorward of its central position, activity likely began hours earlier still. The potential for measuring Doppler shifts of H_3^+ lines was assessed: $R \sim 25{,}000$ provides 12 km s^{-1} per pixel, or 1.2 km s^{-1} with 0.1 pixel precision. However, the signal-to-noise ratio was insufficient for the required accuracy to detect these velocities.

The velocities we report at lower longitudes align well with the 0.62 km s^{-1} velocity average reported by O'Donoghue et al. (2021), but the overall average and high longitude values here are much larger. In other Jovian observations, velocities of approximately 2 km s^{-1} have been recorded within the auroral region, comparable with the faster flows seen here (Wang et al., 2023). At Earth, Nykiel et al. (2024) report velocities for LSTIDs on the order of 0.5–1.6 km s^{-1}, which span most of the range of velocities seen here at Jupiter. Modeling work demonstrates westward zonal flows between 0.5 and 1.2 km s^{-1} far away in the thermosphere's sub-auroral region (Bougher et al., 2005), but Yates et al. (2014) modeled meridional flows of just 0.18 km s^{-1} in response to solar wind compression. From our observations, it remains unclear to what extent this hot feature is carried by an existing background flow or actively drives it.

Solar wind conditions at Jupiter for the dates surrounding 24 and 25 January were hind-cast in O'Donoghue et al. (2021), using the 1-Dimensional magnetohydrodynamic model Tao-MHD (Tao et al., 2005). A more than ten-fold increase in solar wind dynamic pressure was found near the observations, and such an increase can compress the Jovian magnetosphere substantially, moving the dayside magnetopause from 100 to 50 R_J (Bagenal, 2007). Here, we also add an open-source 1-D hydrodynamic model of the solar wind, called the Heliospheric Upwind eXtrapolation model (time-dependent) (HUXt) Owens et al. (2020); Barnard and Owens (2022), which hind-casts high velocity solar wind streams of ∼650 km s^{-1} impacting the Jovian system on 24–25 January (following typical velocities of ∼400 km s^{-1}), as seen in Movie S1.

During this time, the Juno spacecraft was in Jupiter orbit, providing in-situ insights into magnetospheric activity: data from the Juno Waves instrument is shown in Figure 3 (Kurth et al., 2017). Overlain on this figure, in all panels, is the full range of launch times (derived above) and the Keck observation time range. Trapped continuum radiation, typically observed in the outer magnetosphere, appears between 0.3–5 kHz (panel d), with a low-frequency cutoff at the local plasma frequency proportional to the square root of electron density (panel c). The emission vanishes at the end of 24 January, returning late on 25 January, indicating that Juno exited the magnetosphere into the higher-density magnetosheath and later re-entered it. Indeed, Louis et al. (2023) report that the Juno spacecraft crossed the magnetopause six times in total over a 22-hr period between January 24–25 (listed as magnetopause crossings 118 through 123 in that study). This occurred despite the Juno spacecraft moving 9 R_J closer to the planet on the dawn sector (5:08 Jupiter local time) during January 24–25, demonstrating that the retreating magnetopause overtook the spacecraft and that the Jovian magnetosphere was being compressed by the impinging solar wind at this time.

Arguments in favor of the hot feature being dynamic are compelling. Energy transport from the main auroral ovals in the form of winds is expected even during quiet conditions, but dramatically so following a solar wind compression of the magnetosphere, particularly at Earth in the form of LSTIDs (Nykiel et al., 2024; Palmroth et al., 2021; Yates et al., 2014). If the feature is stationary on the planet, then it is likely induced externally by the inner-magnetosphere via particle precipitation and associated currents which lead to Joule heating (Kurth et al., 2025). Solar wind compressions are known to shift Io's plasma torus, enhancing the dawn-to-dusk electric field in the inner magnetosphere (Murakami et al., 2016). If this electric field connects to the ionosphere along magnetic field lines, it could increase Joule heating through associated currents, and mark the first time that a large-scale heating mechanism outside the aurora has been documented.

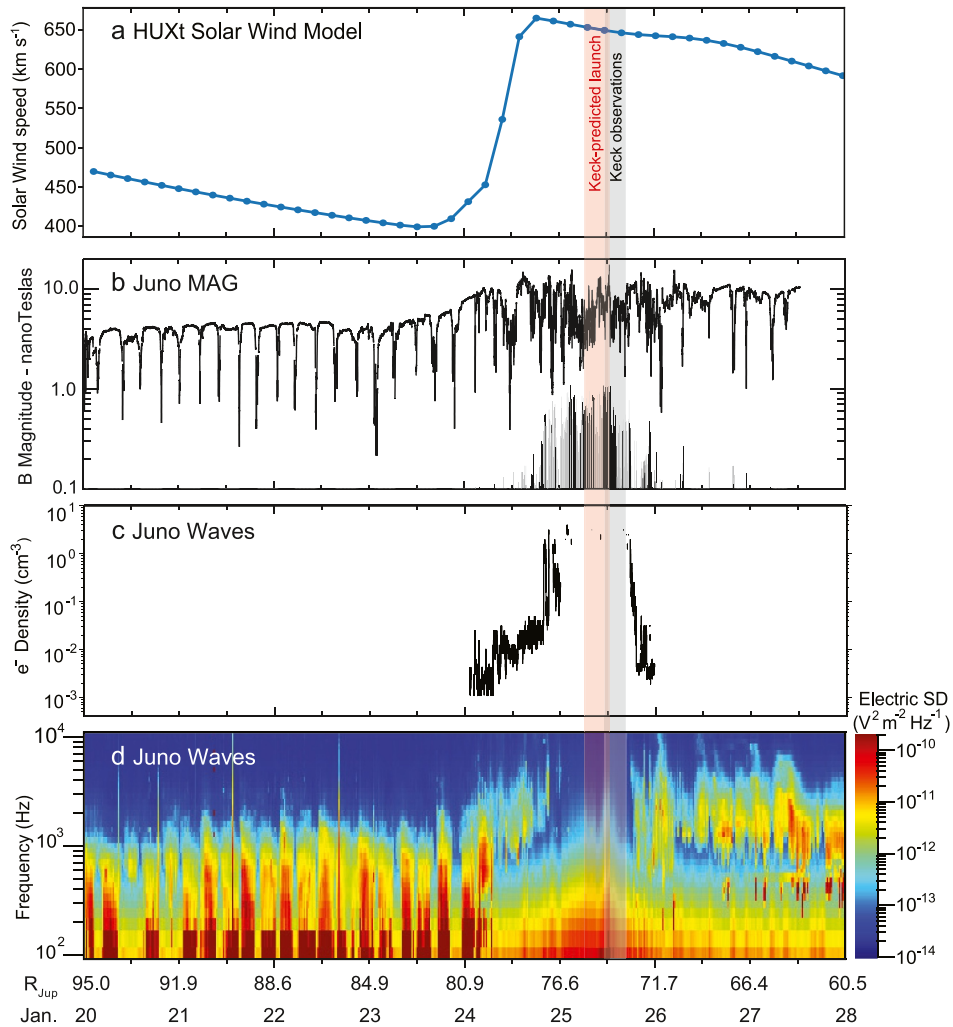

Figure 3. Solar wind propagation modeling at the vicinity of Jupiter with Juno spacecraft instrument data taken in-situ in Jupiter orbit. Panel (a) shows the output of the HUXt solar wind model, illustrating the solar wind speed at Jupiter. Panel (b) presents Juno magnetometer data, showing both the magnetic field magnitude and the root mean square (RMS) fluctuations calculated over 60-s intervals. The RMS fluctuations are in the B_z component of the magnetic field, aligned with the spacecraft's rotation axis (primarily pointed toward Earth), with light shades indicating positive B_z, and darker shades indicating negative B_z. In panel (c), derived electron densities are shown from Juno's Waves instrument (Kurth et al., 2017). Panel (d) shows a time-frequency plot of electric field spectral density, from which the electron density in panel (b) was derived. The *X*-axes show date and Juno spacecraft radial distance (from the center of Jupiter). Overlain are the independently derived Keck launch times for the hot feature, as well as the observations themselves.

4. Conclusions

This study presents a new analysis of Jupiter's upper atmosphere observations taken by the Keck II telescope on 25 January 2017, in which an anomalous hot feature extending over approximately 180° longitude and several degrees of latitude was present. The hot feature is significantly displaced from both the modeled main auroral oval and regions of elevated H_3^+ column density typically associated with auroral precipitation, and reaches temperatures of up to 950 K on top of the surrounding atmospheric background of approximately 750 K.

We explored the hypothesis that the feature was dynamically transported equatorward from the main auroral oval by thermospheric winds, launched after a solar wind-induced compression of the Jovian magnetosphere, analogous to LSTIDs at Earth. Supporting evidence includes the derivation of a realistic mean flow velocity of 1.1 ± 0.2 km s^{-1}, which aligns with the central (hottest) part of the feature having left main oval on average at 10:24 UT, though the feature has a wide range of velocities in longitude. The derived velocities likely correspond

19448007, 2025, 7, Downloaded from https://agupubs.onlinelibrary.wiley.com/doi/10.1029/2024GL113751 by Test, Wiley Online Library on [05/04/2025]. See the Terms and Conditions (https://onlinelibrary.wiley.com/terms-and-conditions) on Wiley Online Library for rules of use; OA articles are governed by the applicable Creative Commons License

19448007, 2025, 7, Downloaded from https://agupubs.onlinelibrary.wiley.com/doi/10.1029/2024GL113751 by Test, Wiley Online Library on [05/04/2025]. See the Terms and Conditions (https://onlinelibrary.wiley.com/terms-and-conditions) on Wiley Online Library for rules of use; OA articles are governed by the applicable Creative Commons License

to the feature's own velocity mixed with that of the background wind field, but the relative contributions are unknown. Two solar wind models predict high pressure, fast streams arrive at Jupiter in the days surrounding the observation, and the Juno spacecraft detected characteristic signatures of magnetospheric compression from several hours prior to the observations. These facts imply that, if the high temperature feature results from magnetospheric compression, hot thermospheric flows began escaping from the main oval as soon as the magnetosphere started being compressed.

We also considered the possibility that the hot feature is stationary, imposed by inner magnetosphere-ionosphere coupling. This could potentially be linked to enhanced dawn-to-dusk electric fields in the inner magnetosphere following solar wind compressions. While some particle precipitation (and energy) must be deposited to the upper atmosphere at mid-latitudes (Kurth et al., 2025), the magnitude of energy required for heating is non-trivial, and without precedent. First; these are auroral-like temperatures over an area larger than the auroral oval, and second; these high temperatures may be sustained over several hours, as they were present during most of the observation window on 25 Jan.

Jupiter's UV aurorae and the solar wind have previously exhibited a complex and variable coupling process that affects auroral brightness and structure (Kita et al., 2016; Nichols et al., 2007). Our findings highlight that the solar wind plays a significant role in the thermal and possibly dynamic behavior of Jupiter's upper atmosphere, outside of the auroral regions. Future observations, ideally conducted over consecutive Jovian rotations, will definitively determine whether hot features like the one identified are migrating equatorward. Concurrently, theoretical studies may uncover new mechanisms for energy delivery within the innermost magnetosphere. Regardless of the underlying cause of the additional heat in this region, our analysis suggests that the solar wind is the most probable root cause, with profound consequences for global thermal energy balance.

Data Availability Statement

Telescopic data (spectra and guider images) are publicly available in a raw FITS format on https://nexsci.caltech.edu/archives/koa/. Open-source computer code used for fitting to H_3^+ and producing temperatures, densities and radiances is available in the Python programming language at https://pypi.org/project/h3ppy/. Results from the work presented here are available and stored as IDL .sav files with temperature, density and radiance as a function of longitude and latitude, along with their uncertainties, together with longitude, latitude and L-shell mappings for the hot feature (O'Donoghue, 2025). The Juno Waves data used in this paper are available from NASA's Planetary Data System (Kurth, 2021). Open-source JupiterMag Python code was used to perform magnetic field-line tracing from the planet to the equatorial plane (version 1.3.1, to degree 13) (Wilson et al., 2023). Open-source HUXt code was used in propagating the solar wind at out to Jupiter (version 4.2.0) (Barnard & Owens, 2022).

Acknowledgments

J.O. was supported by the STFC Ernest Rutherford Fellowship ST/X003426/1 at the University of Reading and the Japanese Space Agency under the International Top Young Fellow programme. L.M. was supported by NASA under Grant NNX17AF14G issued through the Solar System Observations Program and Grant 80NSSC19K0546 issued through the Solar System Workings Program. H.M. was supported by the STFC James Webb Fellowship ST/W001527/1. T.S.S. was supported by UK STFC Consolidated Grant ST/W00089X/1. W.S.K.'s research at the University of Iowa is supported by NASA through Contract 699041X with the Southwest Research Institute. W.S.K. acknowledges the use of the Space Physics Data Repository at the University of Iowa supported by the Roy J. Carver Charitable Trust. P.I.T. was funded by STFC Studentship ST/X508548/2. K.L.K. was supported by a Northumbria University Research Studentship at Northumbria University, UK. O.A. was funded by NASA Grant 80NSSC21K0157 (Solar System Workings Program) and NASA Grant 80NSSC23K0661 (New Frontiers Data Analysis Program). R.W. was supported by a University of Leicester Doctoral Scholarship. The data presented herein were obtained at the W.M. Keck Observatory, which is operated as a scientific partnership among the California Institute of Technology, the University of California and NASA. The Observatory was made possible by the generous financial support of the W.M. Keck Foundation. The authors wish to recognize and acknowledge the cultural role and reverence that the summit of Maunakea has always had within the indigenous Hawaiian community. We are fortunate to have the opportunity to conduct observations from this mountain. This research was supported by the International Space Science Institute for the international team on "Jupiter's Non-Auroral Ionosphere."

References

Adriani, A., Mura, A., Moriconi, M. L., Dinelli, B. M., Fabiano, F., Altieri, F., et al. (2017). Preliminary JIRAM results from Juno polar observations: 2. Analysis of the Jupiter southern H^{3+} emissions and comparison with the north aurora. *Geophysical Research Letters*, *44*(10), 4633–4640. https://doi.org/10.1002/2017GL072905

Bagenal, F. (2007). The magnetosphere of Jupiter: Coupling the equator to the poles. *Journal of Atmospheric and Solar-Terrestrial Physics*, *69*(3), 387–402. https://doi.org/10.1016/j.jastp.2006.08.012

Barnard, L., & Owens, M. (2022). HUXt—An open source, computationally efficient reduced-physics solar wind model, written in Python (Version 4.2.0) [Software]. *Frontiers in Physics*, *10*. https://doi.org/10.3389/fphy.2022.1005621.1005621.

Baron, R. L., Owen, T., Connerney, J. E. P., Satoh, T., & Harrington, J. (1996). Solar wind control of Jupiter's H^{3+} auroras. *Icarus*, *120*(2), 437–442. https://doi.org/10.1006/icar.1996.0063

Bonfond, B., Yao, Z., & Grodent, D. (2020). Six pieces of evidence against the corotation enforcement theory to explain the main aurora at Jupiter. *Journal of Geophysical Research: Space Physics*, *125*(11), e28152. https://doi.org/10.1029/2020JA028152

Borries, C., Jakowski, N., Kauristie, K., Amm, O., Mielich, J., & Kouba, D. (2017). On the dynamics of large-scale traveling ionospheric disturbances over Europe on 20 November 2003. *Journal of Geophysical Research: Space Physics*, *122*(1), 1199–1211. https://doi.org/10.1002/2016JA023050

Bougher, S. W., Waite, J. H., Majeed, T., & Gladstone, G. R. (2005). Jupiter Thermospheric General Circulation Model (JTGCM): Global structure and dynamics driven by auroral and Joule heating. *Journal of Geophysical Research: Planets*, *110*(E4), E04008. https://doi.org/10.1029/2003JE002230

Connerney, J. E. P., Kotsiaros, S., Oliversen, R. J., Espley, J. R., Joergensen, J. L., Joergensen, P. S., et al. (2018). A new model of Jupiter's magnetic field from Juno's first nine orbits. *Geophysical Research Letters*, *45*(6), 2590–2596. https://doi.org/10.1002/2018GL077312

Connerney, J. E. P., Timmins, S., Herceg, M., & Joergensen, J. L. (2020). A Jovian magnetodisc model for the Juno Era. *Journal of Geophysical Research: Space Physics*, *125*(10), e28138. https://doi.org/10.1029/2020JA028138

Connerney, J. E. P., Timmins, S., Oliversen, R. J., Espley, J. R., Joergensen, J. L., Kotsiaros, S., et al. (2022). A new model of Jupiter's magnetic field at the completion of Juno's Prime Mission. *Journal of Geophysical Research: Planets*, *127*(2), e07055. https://doi.org/10.1029/2021JE007055

Cowley, S. W. H., Alexeev, I. I., Belenkaya, E. S., Bunce, E. J., Cottis, C. E., Kalegaev, V. V., et al. (2005). A simple axisymmetric model of magnetosphere-ionosphere coupling currents in Jupiter's polar ionosphere. *Journal of Geophysical Research*, *110*(A11), 11209. https://doi.org/10.1029/2005JA011237

Gladstone, G. R., Persyn, S. C., Eterno, J. S., Walther, B. C., Slater, D. C., Davis, M. W., et al. (2017). The ultraviolet spectrograph on NASA's Juno Mission. *Space Science Reviews*, *213*(1–4), 447–473. https://doi.org/10.1007/s11214-014-0040-z

Johnson, R. E., Melin, H., Stallard, T. S., Tao, C., Nichols, J. D., & Chowdhury, M. N. (2018). Mapping H^{3+} temperatures in Jupiter's northern auroral ionosphere using VLT-CRIRES. *J. Geophys. Res.: Space Physics*, *123*(7), 5990–6008. https://doi.org/10.1029/2018JA025511

Karney, C. F. F. (2013). Algorithms for geodesics. *Journal of Geodesy*, *87*(1), 43–55. https://doi.org/10.1007/s00190-012-0578-z

Kita, H., Kimura, T., Tao, C., Tsuchiya, F., Misawa, H., Sakanoi, T., et al. (2016). Characteristics of solar wind control on Jovian UV auroral activity deciphered by long-term Hisaki EXCEED observations: Evidence of preconditioning of the magnetosphere? Geophys. *Research Letters*, *43*(13), 6790–6798. https://doi.org/10.1002/2016GL069481

Kurth, W. S. (2021). Juno E/j/ss waves calibrated survey full resolution V2.0 [Dataset]. NASA Planetary Data System, JNO-E/J/SS-WAV-3-CDR-SRVFULL-V2.0. https://doi.org/10.17189/1520498

Kurth, W. S., Faden, J. B., Waite, J. H., Sulaiman, A. H., Elliott, S. S., Hospodarsky, G. B., et al. (2025). Electron densities in Jupiter's upper ionosphere inferred from Juno plasma wave observations. *Journal of Geophysical Research: Planets*, *130*, e2024JE008845. https://doi.org/10.1029/2024JE008845

Kurth, W. S., Imai, M., Hospodarsky, G. B., Gurnett, D. A., Louarn, P., Valek, P., et al. (2017). A new view of Jupiter's auroral radio spectrum. *Geophysical Research Letters*, *44*(14), 7114–7121. https://doi.org/10.1002/2017GL072889

Lam, H. A., Achilleos, N., Miller, S., Tennyson, J., Trafton, L. M., Geballe, T. R., & Ballester, G. E. (1997). A baseline spectroscopic study of the infrared auroras of Jupiter. *Icarus*, *127*(2), 379–393. https://doi.org/10.1006/icar.1997.5698

Lian, Y., & Yelle, R. V. (2019). Damping of gravity waves by kinetic processes in Jupiter's thermosphere. *Icarus*, *329*, 222–245. https://doi.org/10.1016/j.icarus.2019.04.001

Louis, C. K., Jackman, C. M., Hospodarsky, G., O'Kane Hackett, A., Devon-Hurley, E., Zarka, P., et al. (2023). Effect of a magnetospheric compression on Jovian radio emissions: In situ case study using Juno data. *Journal of Geophysical Research: Space Physics*, *128*(9), e2022JA031155. https://doi.org/10.1029/2022JA031155

Matcheva, K. I., & Strobel, D. F. (1999). Heating of Jupiter's thermosphere by dissipation of gravity waves due to molecular viscosity and heat conduction. *Icarus*, *140*(2), 328–340. https://doi.org/10.1006/icar.1999.6151

McLean, I. S., Becklin, E. E., Bendiksen, O., Brims, G., Canfield, J., Figer, D. F., et al. (1998). Design and development of NIRSPEC: A near-infrared echelle spectrograph for the Keck II telescope. In A. M. Fowler (Ed.), *Infrared astronomical instrumentation* (Vol. 3354, pp. 566–578). https://doi.org/10.1117/12.317283

Melin, H., Badman, S., & Khurana, K. (2016). The 2013 Saturn auroral campaign. *Icarus*, *263*, 1. https://doi.org/10.1016/j.icarus.2015.09.028

Melin, H., Miller, S., Stallard, T., Smith, C., & Grodent, D. (2006). Estimated energy balance in the Jovian upper atmosphere during an auroral heating event. *Icarus*, *181*(1), 256–265. https://doi.org/10.1016/j.icarus.2005.11.004

Melin, H., O'Donoghue, J., Moore, L., Stallard, T. S., Fletcher, L. N., Roman, M. T., et al. (2024). Ionospheric irregularities at Jupiter observed by JWST. *Nature Astronomy*, *8*, 1000–1007. https://doi.org/10.1038/s41550-024-02305-9

Melin, H., Stallard, T. S., O'Donoghue, J., Badman, S. V., Miller, S., & Blake, J. S. D. (2014). On the anticorrelation between H^{3+} temperature and density in giant planet ionospheres. *Monthly Notices of the Royal Astronomical Society*, *438*(2), 1611–1617. https://doi.org/10.1093/mnras/stt2299

Migliorini, A., Dinelli, B. M., Moriconi, M. L., Altieri, F., Adriani, A., Mura, A., et al. (2019). H^{3+} characteristics in the Jupiter atmosphere as observed at limb with Juno/JIRAM. *Icarus*, *329*, 132–139. https://doi.org/10.1016/j.icarus.2019.04.003

Miller, S., Stallard, T., Melin, H., & Tennyson, J. (2010). H^{3+} cooling in planetary atmospheres. *Faraday Discussions*, *147*, 283–291. https://doi.org/10.1039/c004152c

Miller, S., Stallard, T., Smith, C., Millward, G., Melin, H., Lystrup, M., & Aylward, A. (2006). H^{3+}: The driver of giant planet atmospheres. *Philosophical Transactions of the Royal Society of London*, *364*(1848), 3121–3137. https://doi.org/10.1098/rsta.2006.1877

Miller, S., Tennyson, J., Geballe, T. R., & Stallard, T. (2020). Thirty years of H^{3+} astronomy. *Reviews of Modern Physics*, *92*(3), 035003. https://doi.org/10.1103/RevModPhys.92.035003

Moore, L., O'Donoghue, J., Melin, H., Stallard, T., Tao, C., Zieger, B., et al. (2017). Variability of Jupiter's IR H^{3+} aurorae during Juno approach. *Geophysical Research Letters*, *44*(10), 4513–4522. https://doi.org/10.1002/2017GL073156

Murakami, G., Yoshioka, K., Yamazaki, A., Tsuchiya, F., Kimura, T., Tao, C., et al. (2016). Response of Jupiter's inner magnetosphere to the solar wind derived from extreme ultraviolet monitoring of the Io plasma torus. *Geophysical Research Letters*, *43*(24), 12308–12316. https://doi.org/10.1002/2016GL071675

Nichols, J. D., Bunce, E. J., Clarke, J. T., Cowley, S. W. H., Gérard, J. C., Grodent, D., & Pryor, W. R. (2007). Response of Jupiter's UV auroras to interplanetary conditions as observed by the Hubble Space Telescope during the Cassini flyby campaign. *Journal of Geophysical Research: Space Physics*, *112*(A2), A02203. https://doi.org/10.1029/2006JA012005

Nykiel, G., Ferreira, A., Günzkofer, F., Iochem, P., Tasnim, S., & Sato, H. (2024). Large-scale traveling ionospheric disturbances over the European sector during the geomagnetic storm on March 23-24, 2023: Energy deposition in the source regions and the propagation characteristics. *Journal of Geophysical Research: Space Physics*, *129*(3), e2023JA032145. https://doi.org/10.1029/2023JA032145

O'Donoghue, J. (2025). Dataset for paper: Sub-auroral heating at Jupiter following a solar wind compression [Dataset]. *Zenodo*. https://doi.org/10.5281/zenodo.14061030

O'Donoghue, J., Moore, L., Bhakyapaibul, T., Melin, H., Stallard, T., Connerney, J. E. P., & Tao, C. (2021). Global upper-atmospheric heating on Jupiter by the polar aurorae. *Nature*, *596*(7870), 54–57. https://doi.org/10.1038/s41586-021-03706-w

O'Donoghue, J., Moore, L., Stallard, T. S., & Melin, H. (2016). Heating of Jupiter's upper atmosphere above the Great Red Spot. *Nature*, *536*(7615), 190–192. https://doi.org/10.1038/nature18940

O'Donoghue, J., & Stallard, T. (2022). What the upper atmospheres of giant planets reveal. *Remote Sensing*, *14*(24), 6326. https://doi.org/10.3390/rs14246326

O'Donoghue, J., Stallard, T. S., Melin, H., Cowley, S. W. H., Badman, S. V., Moore, L., et al. (2014). Conjugate observations of Saturn's northern and southern H^{3+} aurorae. *Icarus*, *229*, 214–220. https://doi.org/10.1016/j.icarus.2013.11.009

Owens, M., Lang, M., Barnard, L., Riley, P., Ben-Nun, M., Scott, C. J., et al. (2020). A computationally efficient, time-dependent model of the solar wind for use as a surrogate to three-dimensional numerical magnetohydrodynamic simulations. *Solar Physics*, *295*(3), 43. https://doi.org/10.1007/s11207-020-01605-3

Palmroth, M., Grandin, M., Sarris, T., Doornbos, E., Tourgaidis, S., Aikio, A., et al. (2021). Lower-thermosphere-ionosphere (LTI) quantities: Current status of measuring techniques and models. *Annales Geophysicae*, *39*(1), 189–237. https://doi.org/10.5194/angeo-39-189-2021

19448007, 2025, 7, Downloaded from https://agupubs.onlinelibrary.wiley.com/doi/10.1029/2024GL113751 by Test, Wiley Online Library on [05/04/2025]. See the Terms and Conditions (https://onlinelibrary.wiley.com/terms-and-conditions) on Wiley Online Library for rules of use; OA articles are governed by the applicable Creative Commons License

Smith, C. G. A., Aylward, A. D., Millward, G. H., Miller, S., & Moore, L. E. (2007). An unexpected cooling effect in Saturn's upper atmosphere. *Nature*, *445*(7126), 399–401. https://doi.org/10.1038/nature05518

Stallard, T., Miller, S., Millward, G., & Joseph, R. D. (2001). On the dynamics of the Jovian ionosphere and thermosphere. I. The measurement of ion winds. *Icarus*, *154*(2), 475–491. https://doi.org/10.1006/icar.2001.6681

Stallard, T. S., Burrell, A. G., Melin, H., Fletcher, L. N., Miller, S., Moore, L., et al. (2018). Identification of Jupiter's magnetic equator through H^{3+} ionospheric emission. *Nature Astronomy*, *2*(10), 773–777. https://doi.org/10.1038/s41550-018-0523-z

Strobel, D. F., & Smith, G. R. (1973). On the temperature of the Jovian thermosphere. *Journal of the Atmospheric Sciences*, *30*, 718–725. https://doi.org/10.1175/1520-0469(1973)

Tao, C., Badman, S. V., & Fujimoto, M. (2011). UV and IR auroral emission model for the outer planets: Jupiter and Saturn comparison. *Icarus*, *213*(2), 581–592. https://doi.org/10.1016/j.icarus.2011.04.001

Tao, C., Kataoka, R., Fukunishi, H., Takahashi, Y., & Yokoyama, T. (2005). Magnetic field variations in the Jovian magnetotail induced by solar wind dynamic pressure enhancements. *Journal of Geophysical Research*, *110*(A11), A11208. https://doi.org/10.1029/2004JA010959

Walterscheid, R. L., Schubert, G., & Brinkman, D. G. (2003). Acoustic waves in the upper mesosphere and lower thermosphere generated by deep tropical convection. *Journal of Geophysical Research*, *108*(A11), 1392. https://doi.org/10.1029/2003JA010065

Wang, R., Stallard, T. S., Melin, H., Baines, K. H., Achilleos, N., Rymer, A. M., et al. (2023). Asymmetric ionospheric jets in Jupiter's aurora. *Journal of Geophysical Research: Space Physics*, *128*(12), e2023JA031861. https://doi.org/10.1029/2023JA031861

Wilson, R. J., Vogt, M. F., Provan, G., Kamran, A., James, M. K., Brennan, M., & Cowley, S. W. H. (2023). Internal and external Jovian magnetic fields: Community code to serve the magnetospheres of the outer planets community (version 1.3.1, to degree 13) [Software]. *Space Science Reviews*, *219*(1), 15. https://doi.org/10.1007/s11214-023-00961-3

Yates, J. N., Achilleos, N., & Guio, P. (2014). Response of the Jovian thermosphere to a transient pulse in solar wind pressure. *Planetary and Space Science*, *91*, 27–44. https://doi.org/10.1016/j.pss.2013.11.009

Yates, J. N., Ray, L. C., Achilleos, N., Witasse, O., & Altobelli, N. (2020). Magnetosphere-ionosphere-thermosphere coupling at Jupiter using a three-dimensional atmospheric general circulation model. *Journal of Geophysical Research: Space Physics*, *125*(1), e26792. https://doi.org/10.1029/2019JA026792

Yelle, R. V., & Miller, S. (2004). Jupiter's thermosphere and ionosphere. In *Jupiter. the planet, satellites and magnetosphere* (pp. 185–218). Cambridge University Press.

19448007, 2025, 7, Downloaded from https://agupubs.onlinelibrary.wiley.com/doi/10.1029/2024GL113751 by Test, Wiley Online Library on [05/04/2025]. See the Terms and Conditions (https://onlinelibrary.wiley.com/terms-and-conditions) on Wiley Online Library for rules of use; OA articles are governed by the applicable Creative Commons License